N91-21189

MAGNETIC SUSPENSION SYSTEMS for SPACE APPLICATIONS

Douglas G. Havenhill, Patrick J. Wolke

Honeywell Incorporated

Satellite Systems Operations

19019 North 59th Avenue

Glendale

AZ 85308-9650

INTRODUCTION

History

For over 20 years Honeywell Inc., Satellite Systems Operations in Glendale, Arizona, has designed, built, and tested magnetic suspensions for bearing systems and for vibration isolation and precision pointing of spaceborne equipment. Starting in the 1970s, with the development of momentum wheel bearings and the Advanced Vernier System (AVS), Honeywell has designed, built, and tested systems ranging from magnetic bearings for a small optical scanner to a six-degree-of-freedom magnetic suspension that requires six 3200-Newton actuators to rapidly retarget a large optical telescope while maintaining precision isolation.

The magnetic actuator has evolved to a high-bandwidth, low-power, precision linear force device that can be optimally arranged in a system to provide better than 80 dB of isolation in all six degrees of freedom. The active control structure permits flexibility in configuring systems to support a wide variety of payloads and to tailor the responses of the system. As an example, systems have been built that isolate a payload in the translational degrees of freedom while precisely pointing and isolating it in the rotational degrees of freedom. Our broad range of experience makes Honeywell a leader in the spaceborne magnetic suspension field. This paper provides an overview of the techniques used in our magnetic suspension systems and a review of the systems already developed, which demonstrate the usefulness, applicability, and flight readiness of magnetic suspension to a broad range of payloads and environments.

Programs

Table 1 provides a brief synopsis of selected magnetic isolation and pointing system programs that have been worked at Honeywell. The AVS, developed for the National Aeronautics and Space Administration (NASA) Langley Research Center (LaRC), demonstrated 0.03-arc-second pointing stability in the presence of simulated Shuttle reaction jet disturbances.

The Annular Suspension and Pointing System (ASPS), shown in Figure 1, was the first major magnetic isolation and pointing system developed for spaceborne payloads by Honeywell Inc., Satellite Systems Operations. The ASPS is composed of a two-axis course gimbal system, known as the Advanced Gimbal System (AGS), and the magnetic pointing and isolation system, known as the Advanced Vernier System (AVS).

The AVS is a six-degree-of-freedom magnetic suspension system that is situated atop the two-gimbal course-pointing system. It is designed to provide isolation of payloads from space shuttle disturbances, as well as to provide pointing stability and vernier control much better than the gimbal system alone [1, 2, 3, 4, 5, 6, 7, 8, 9]. The ASPS control system was designed to operate the gimbals in a follow-up mode to the AVS for large rotations. A more detailed view of the AVS engineering model, which was developed and tested, is shown in Figure 2. A unique feature of this device is its ability to provide full 360 degrees of rotation in roll. The armature is a continuous ring with an L-shaped cross-section; three magnetic actuators apply force axially and three apply force radially. Actuator stabilization was achieved with gap feedback control. Roll control was achieved with an AC induction motor and a roll resolver.

Table 1. Honeywell Magnetic Suspension Systems Background

Dates	Customer	Description
1976 - 1984	NASA LaRC	Contract to design, build, and lab test a magnetically suspended experiment pointing system for the shuttle AVS.
1977 - 1980	NASA LaRC	Contract to complete development and lab test of a magnetically suspended Annular Momentum Control Device (AMCD).
1984 - 1986	NASA LaRC	Contract to study an advanced AMCD for Space Station power and control.
1985 - 1986	Internal Research and Development (IR&D)	Develop, build, and lab test ISODRIVE, a magnetically suspended vibration isolating gimbal.
1985 - 1986	IR&D	Develop, build, and lab test Fluid Experiment Apparatus Magnetic Isolation System (FEAMIS), a magnetic isolation system for the Fluid Experiment Apparatus, planned to fly on the Shuttle.
1986 - 1987	NASA Ames Research Center (ARC)	Contract to study passive and active magnetic isolation and pointing systems for the Astrometric Telescope Facility (ATF) on the Space Station.

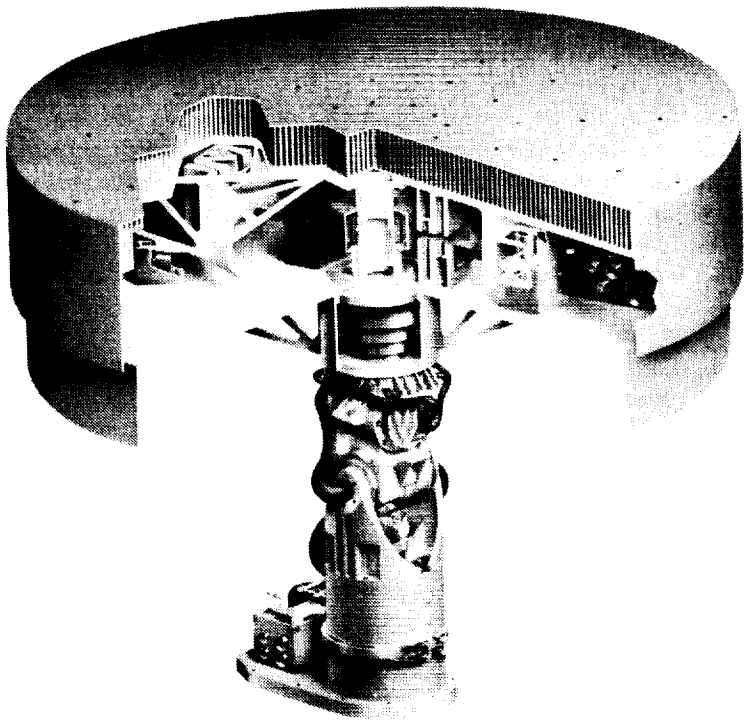

Figure 1. Annular Suspension and Pointing System

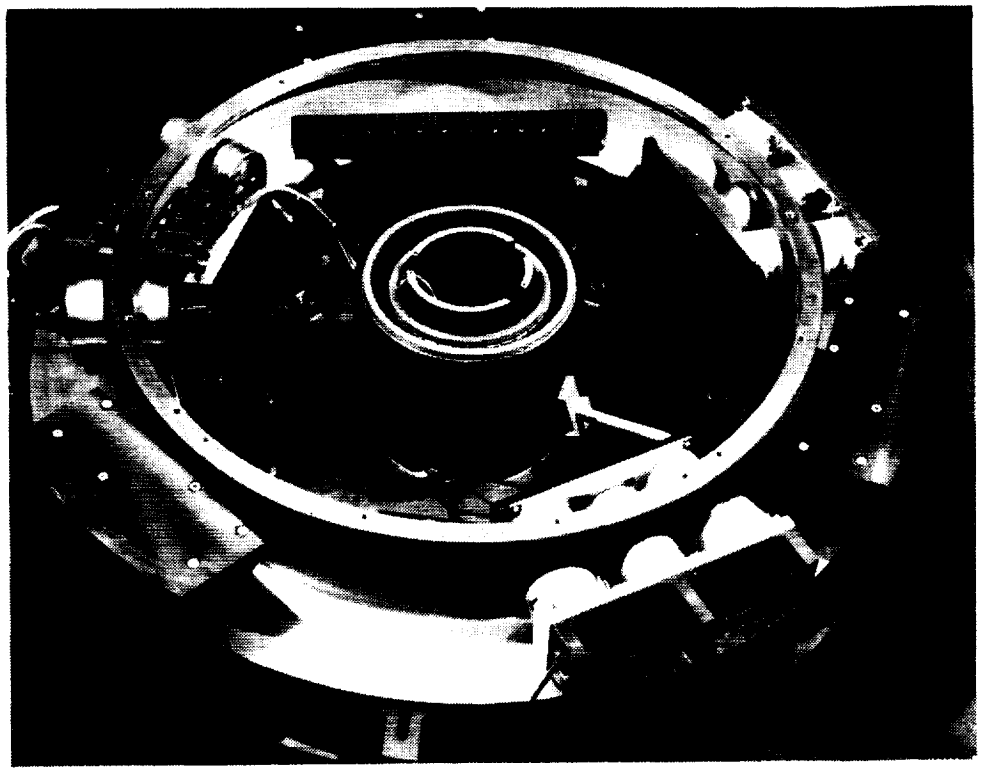

Figure 2. Laboratory Magnetic Isolation and Pointing System ASPS Vernier

A key feature of any isolation system for active payloads is its ability to provide power and signal services across the isolation gap to the payload, without compromising the isolator. For the AVS, power transfer to the payload was achieved with a large-gap, noncontacting power transformer located on the AVS center. This device was developed and tested and provided up to 2.5 kilowatts of power with extremely low disturbance forces. Concepts for large-range-of-motion optical data couplers were also considered.

With the advent of the Shuttle, interest in materials processing in space began to rise. Continuous disturbance levels greater than 0.1 μg are thought to cause significant degradation of crystalline structures grown in space. Honeywell responded by developing a magnetic isolation system, shown in Figure 3, for materials-processing applications. This device, originally developed for Rockwell's Fluid Experiment Apparatus Magnetic Isolation System (FEAMIS), was built and tested at Honeywell [10]. FEAMIS provides six-degree-of-freedom isolation with a bandwidth of 3 Hz and ultimate isolation of greater than 60 dB. Based on more recent technology developments, it is feasible to retrofit FEAMIS to achieve isolation bandwidths less than 0.1 Hz.

The envelope of the FEAMIS was constrained to fit within confines of the Shuttle mid-deck locker as shown in Figure 4. The structure was designed to minimize weight requirements by launching and landing with the payload detached. On orbit, an astronaut lowers and attaches the payload to the isolator. Mechanical clamps are included in the system to prevent uncontrolled motions of the payload and payload mounting plate while the FEAMIS is unpowered. The clamps are released by manual cranks readily accessible to the astronaut. The isolator is then powered by a single switch. Power and signal services to the payload are provided by low-stiffness cable harnesses.

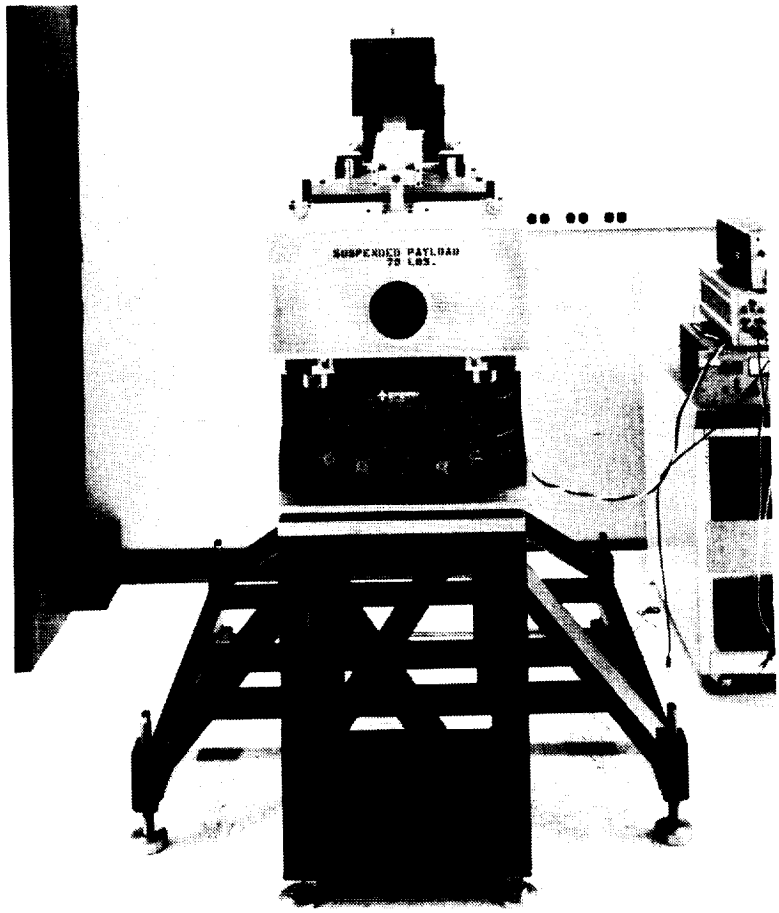

Figure 3. Magnetic Isolator for Materials Processing FEAMIS

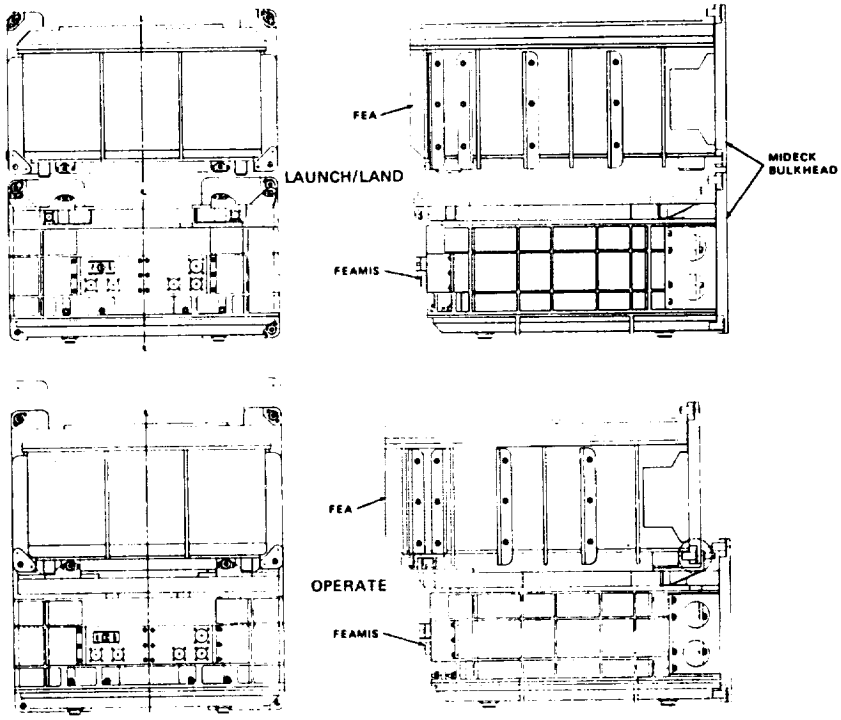

Figure 4. FEAMIS/Payload Attachment

The layout of component hardware within the FEAMIS is shown in Figure 5. The actuators are configured in an axial/tangential array. The armature plates for the tangential actuators are readily seen attached to the payload mounting plate in the lower portion of the photograph. The base structure at the top of the photograph contains the electromagnets, proximity sensors, cages, and all electronics (not shown) necessary for operation of the FEAMIS. This system was the first to use Honeywell's patented flux-feedback approach for control of the magnetic actuators.

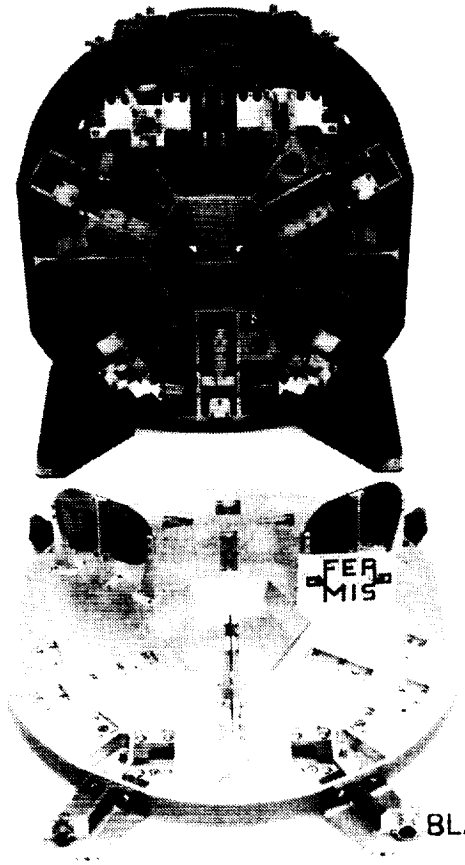

ORIGINAL PAGE
BLACK AND WHITE PHOTOGRAPH

Figure 5. FEAMIS Layout

Accomplishments

Significant accomplishments to date include:

- Demonstration of 0.03-arcsecond pointing stability
- Demonstration of >80-dB isolation
- Demonstration of decoupled pointing and isolation capability
- Demonstration of an all-active six-degree-of-freedom magnetic isolation system
- Demonstration of <0.1-Hz isolation bandwidths

Key Concepts

It is important at this point to define what is meant by the terms pointing and isolation. Pointing refers to the angular positioning of a suspended payload to a commanded angle. This angle could be in some local coordinate system, but more likely a target coordinate system will be used, such as inertial or earth coordinates.

Isolation refers to the reduction in amplitude of base forces transmitted to the suspended payload. Configured as an isolator, magnetic suspension can be likened to a sophisticated six-degree-of-freedom spring, whose spring rate and damping can be independently established for each degree of freedom.

SYSTEM CONSIDERATIONS

To achieve six degrees of freedom of control via one-degree-of-freedom actuators, it can be shown that a minimum set of six actuators is required. There is flexibility in how the actuators are arranged, as long as they do not act through a single point in space. (A singular condition would then exist.) Redundancy may be implemented either by dual coils on each of the six actuators or by an overdetermined set of actuators (e.g., six of eight). Figure 6 illustrates these options.

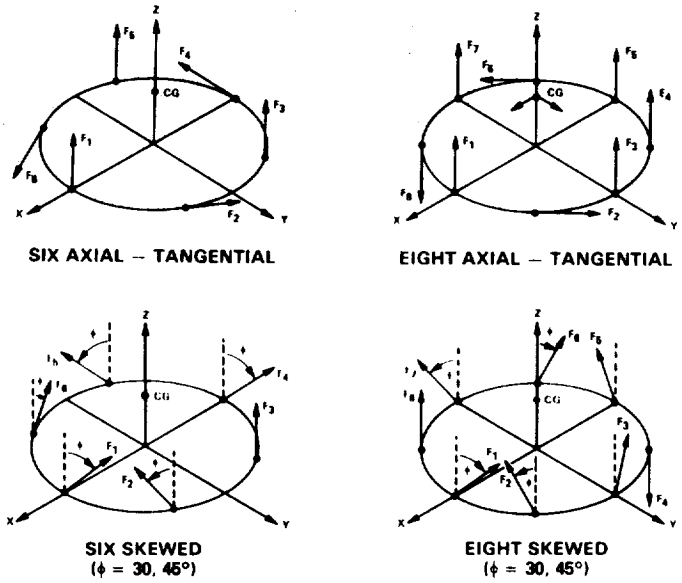

Figure 6. Actuator Configuration Trade-off

The cylindrical (axial-tangential) arrangement of actuators often offers the most compact arrangement of hardware; however, in instances where there is a large asymmetry in the force-torque requirement envelope and/or a large offset of the payload center of gravity (cg) from the centroid of the actuator array, a substantial disparity in the force requirement of the three axial actuators versus the three tangential actuators can exist. This is not an optimal design from a weight and cost standpoint. A skewed arrangement of actuators often resolves the situation, permitting a single, minimum-size actuator to be used. Honeywell has implemented computer optimization routines to quickly and accurately determine optimal arrangements. In some cases, actuator force requirements have been reduced over 50 percent.

Adding dual coils to actuators or adding additional actuators to the array for redundancy will increase weight and power and add redundancy management complexity to the system. Usually a trade study must be performed for the particular system to assess the benefits and drawbacks of each approach; based on the system requirements, a best-design approach can then be selected.

One of the major advantages of the magnetic actuator is its ability to apply force in one direction without constraining motion in any other direction. This unique feature allows a system designer considerable freedom to select a control policy specifically tailored to the payload. To demonstrate this design flexibility, consider a payload suspended by an array of six magnetic actuators. The total force applied to the payload is given by:

$$F = \sum_{i=1}^{6} (d_i F_i) \tag{1}$$

where:
- F = total force applied to payload
- F_i = force delivered by i^{th} actuator
- d_i = a unit vector in the direction of the force

Similarly, the total torque about the payload's center of mass would be:

$$T = \sum_{i=1}^{6} r_i \times (d_i F_i) \tag{2}$$

where:
- T = total torque about center of mass
- r_i = position vector of actuator with respect to center of mass

Writing equations (1) and (2) in matrix form yields:

$$\begin{bmatrix} F \\ T \end{bmatrix} = \begin{bmatrix} d_1 & d_2 & \bullet\bullet\bullet & d_6 \\ r_1 \times d_1 & r_2 \times d_2 & \bullet\bullet\bullet & r_6 \times d_6 \end{bmatrix} \begin{bmatrix} F_1 \\ F_2 \\ \bullet \\ \bullet \\ \bullet \\ F_6 \end{bmatrix} \tag{3}$$

Taking the inverse of the matrix on the right side of equation (3) yields:

$$\begin{bmatrix} F_1 \\ F_2 \\ \bullet \\ \bullet \\ \bullet \\ F_6 \end{bmatrix} = \begin{bmatrix} d_1 & d_2 & \bullet\bullet\bullet & d_6 \\ r_1 \times d_1 & r_2 \times d_2 & \bullet\bullet\bullet & r_6 \times d_6 \end{bmatrix}^{-1} \begin{bmatrix} F_c \\ T_c \end{bmatrix} \tag{4}$$

Now, if the center of mass of the payload is known and the actuators are error free, the above matrix can be implemented in the control law (as shown in Figure 7) to produce forces through and torques about the center of mass. Since the resulting system is completely decoupled, it is possible to tailor the response of each degree of freedom independently. Error-free actuators and certain knowledge of the center-of-mass location are impossible, and these constitute two error sources in magnetic suspension systems. The sensitivity to these errors depends on the relative bandwidths of the control loops used to command the actuators. Minimization of these errors is essential to achieve precision levels of isolation at low frequencies.

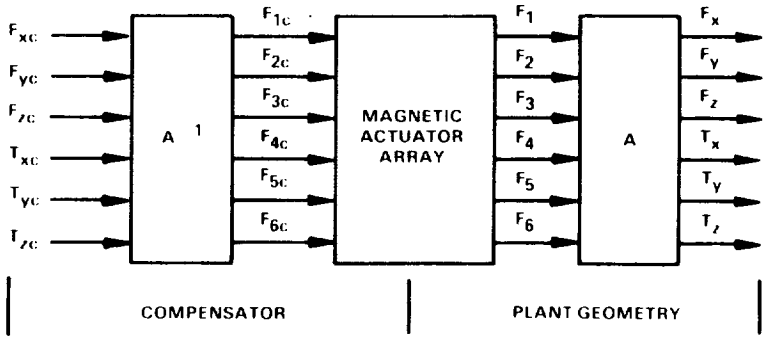

Figure 7. Magnetic Suspension Decoupling Technique

Magnetic Suspension as an Isolator

To use magnetic suspension as an isolator, the relative motion of the payload with respect to the base must be controlled. Rigid-body and low-frequency motion of the base must be followed by the payload, while high-frequency vibrations must not be transmitted to the payload. Usually, in magnetic suspension, the gap between payload and base is measured by proximity sensors mounted at or near the actuator locations; these may be the same proximity sensors used for inner-loop linearization. By combining the six measurements, relative translations and rotations can be determined. Controlling relative motions with low-bandwidth control laws that roll off quickly results in an excellent isolation response. The block diagram of a six-degree-of-freedom isolator is shown in Figure 8. If the payload is nearly rigid, the control compensators can be designed independently and the response of each axis tailored to the disturbance environment expected.

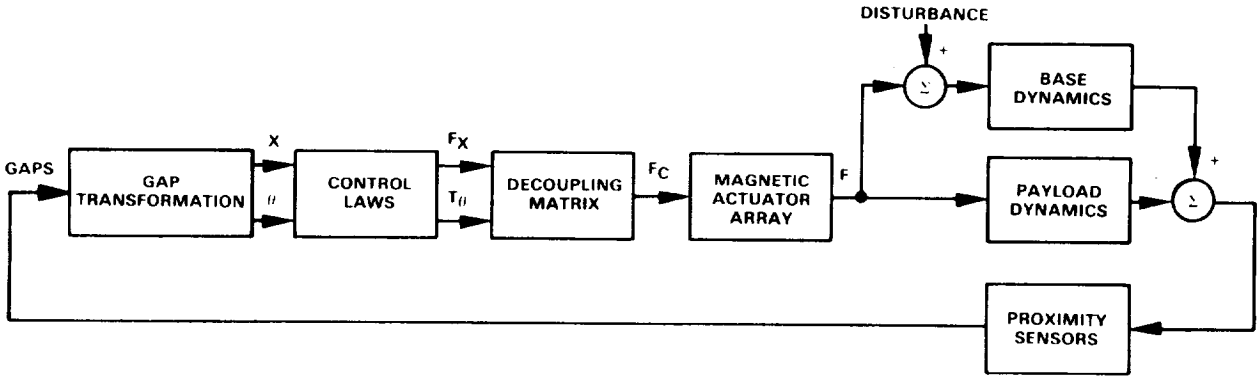

Figure 8. Block Diagram of a Magnetic Suspension Isolator

Magnetic Suspension as a Pointer

If pointing is desired, the translation loops are configured as isolators, and the rotational loops are closed on an inertial sensor. Inertial control also preserves isolation capability but with a different transfer function. Large angles of rotation relative to the base are achieved most effectively by mounting the suspension on top of a gimbal stack and closing the gimbal loops to minimize the relative motion between the payload and the base. This permits

the design of magnetic actuators with reasonably small gaps. Configuring the translational loops as isolators decouples the payload from base vibrations that may corrupt pointing performance [11]. Also, as has recently been proven [15], the soft interface provided by the magnetic suspension ameliorates structural flexibility problems encountered in end-mounted pointers. Figure 9 illustrates the control system structure required for pointing applications.

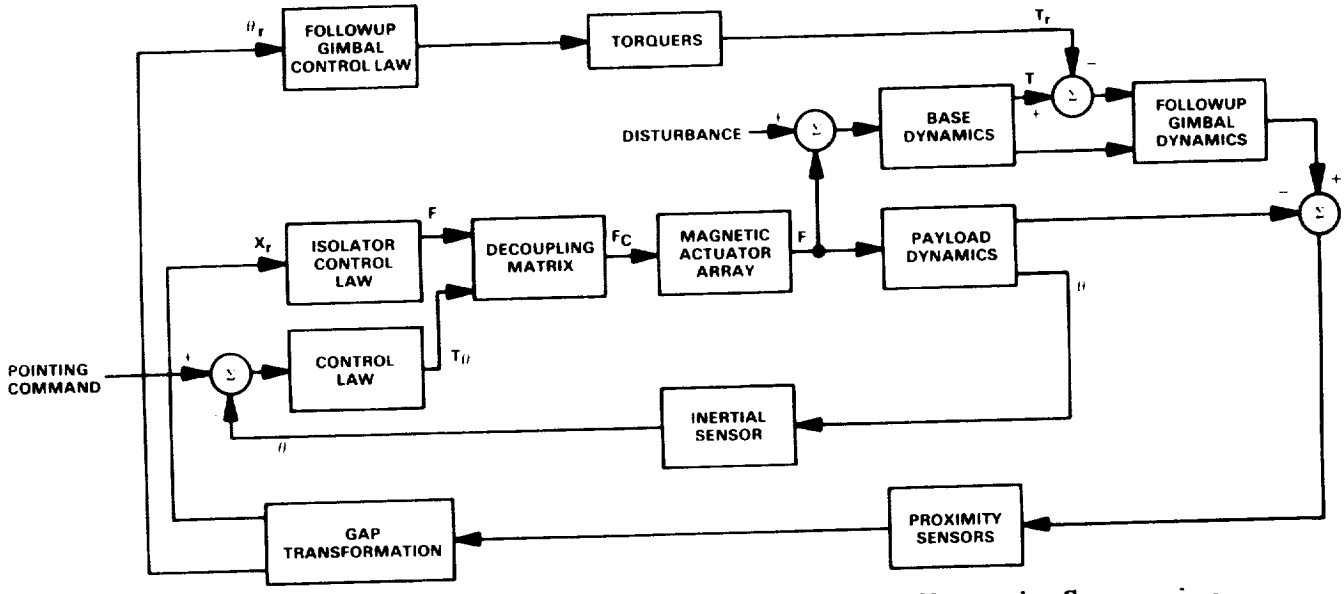

Figure 9. Block Diagram of a Pointing System using Magnetic Suspension

ACTUATOR REQUIREMENTS

To derive the actuator requirements it is necessary to understand the relationship between actuator performance and system performance; in particular, how actuator error sources couple into pointing system and isolation system performance. Generally, magnetic actuator force error sources can be grouped into three categories:

- Errors due to gap motion
- Scale factor errors
- Nonlinearities

This section will describe how these error sources affect pointing and isolation performance.

Pointing Systems

Consider the planar configuration shown in Figure 10. A payload with mass, M, and moment of inertia, J, is suspended in two degrees of freedom with respect of the carrier. Carrier and payload translate only in X, and the payload may rotate through a small angle θ. Figure 11 is a block diagram depicting the structure of the pointing control system for this case. References [11] and [12] contain an excellent derivation of the relationship between carrier motion and pointing error. For our purposes, examining the block diagram yields the following conclusions:

- Scale factor errors in translation become anomalous torque disturbances in the pointing axis.
- Force errors due to gap motion couple into the pointing error.
- Force errors due to nonlinearities also affect the pointing stability.

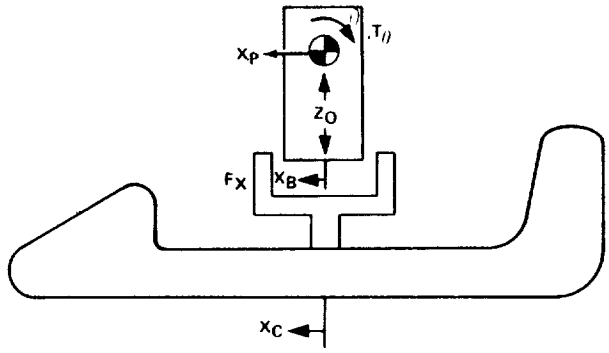

Figure 10. Two-Degree-of-Freedom Example

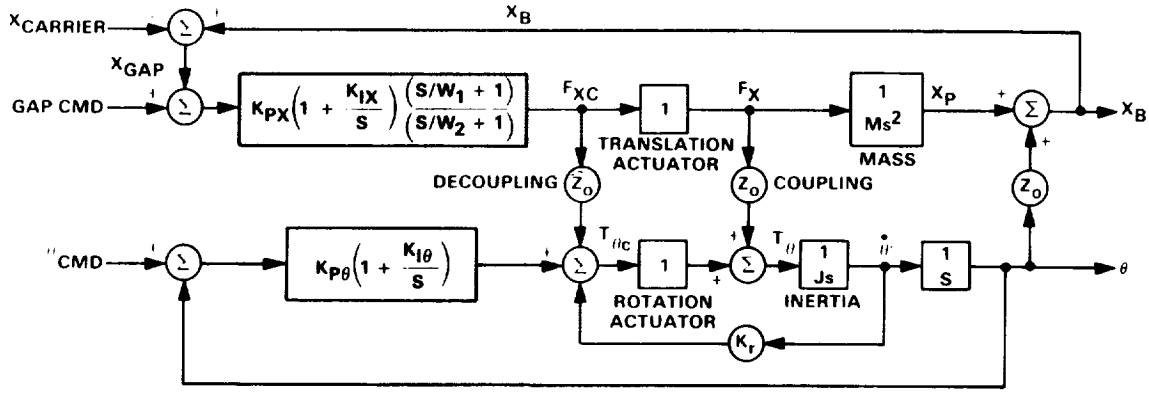

Figure 11. Two-Degree-of-Freedom Block Diagram

The quantitative results of these errors depend on the relative bandwidths of the pointing and isolation sensors; however, pointing systems usually require high-performance, magnetic-force actuators.

Isolation Systems

The goal of an isolation system is to limit the motion of the payload due to carrier motion while allowing the payload to fly with the carrier. In order to accomplish this, a very low-bandwidth (0.01 to 1 Hz) control loop is closed on the gap measurement. Because the system tends to be uncoupled, it can be modeled as six single-degree-of-freedom isolators. Figure 12 illustrates a single-degree-of-freedom system.

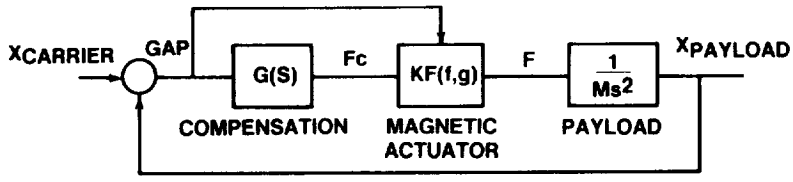

Figure 12. Single-Degree-of-Freedom Isolation System

For this application, scale-factor errors cause slight changes in bandwidth but have negligible impact on pointing performance. Force errors due to gap motion result in dF/dg term, which acts like a mechanical spring shunting the armature to the stator. The effect of this residual spring is to limit low-frequency isolation performance.

Minimizing the appropriate error sources becomes the primary objective of the actuator designer. Techniques for minimizing the error sources include:

- Flux leakage and fringing minimization
- Actuator bandwidth selection
- Actuator control sensor selection

Magnetic Actuator Description

A typical magnetic actuator used in Honeywell suspension devices is shown in Figure 13. This particular actuator was used in the FEAMIS. The actuator consists of two opposing horseshoe electromagnets acting on an armature plate. The electromagnets are mounted to the base, the passive armature is attached to the payload, and they are separated by a large air gap.

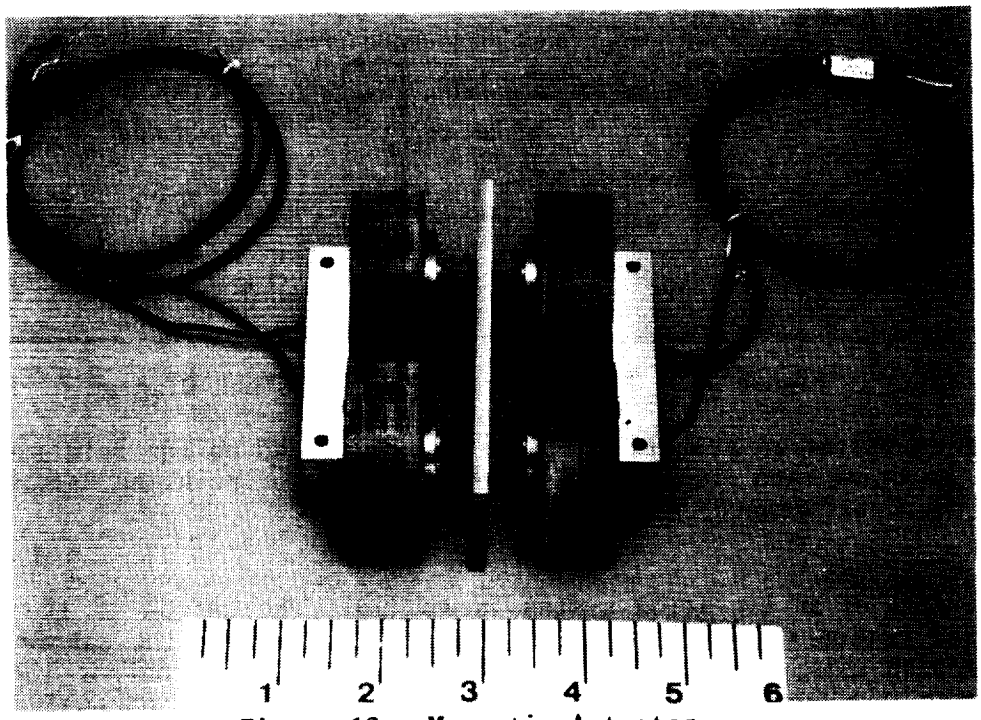

Figure 13. Magnetic Actuator

This type of actuator has been traded against others, such as Lorentz force (voice coil) actuators used for several isolation suspensions at Honeywell. It has repeatedly proved to have better weight and power characteristics, which are key parameters in any space application. Its inductance is much larger than the Lorentz force actuator, and, therefore, it is a poor performer in the high-frequency force regime; however, isolators are rarely required to apply large high-frequency forces, and the Honeywell electromagnet pair design has proved suitable for all applications to date. The large inductance acts to filter voltage driver noise, making this actuator an extremely low-force noise device, which has been substantiated by test data.

Another advantage of the electromagnet pair actuator is its even mass distribution and the fact that the payload attachment can be made entirely passive. The Lorentz force actuator has a large percentage of its mass associated with its permanent magnet (passive) side, and a small mass percentage associated with the coil (active) side. Thus, one is confronted with attaching a large mass to the payload or carrying power to, and dissipating it on, the payload side; both are often undesirable situations. With the electromagnet pair actuator, a reasonably sized passive armature is attached to the payload, and the active electromagnetics are attached to a relatively large base.

The Lorentz force actuator has the advantage of a linear force response to current, whereas the Honeywell actuator is nonlinear. This makes the electronics for the Lorentz force actuator simpler to implement; however, several solutions to the nonlinear force law of the electromagnet pair actuator exist and have been implemented with only some additional complexity.

MAGNETIC ACTUATOR CONTROL TECHNIQUES

Because the force output of an electromagnet is unidirectional and dependent upon the square of the flux linkage or current, controlling the actuator requires some circuitry to control output. One way to do this is to examine the sign of the command, take the square root of the magnitude of the command, and apply current the appropriate coil. This technique requires square-root electronics, which are sensitive and poorly behaved, and inherently have a dead band around zero force. A number of different techniques for controlling the magnetic actuator have been developed and used by Honeywell. This section will describe these techniques and emphasize the relative advantages and disadvantages of each technique.

- Gap/Current Feedback
  - Technique

    One way to control the actuator force is to modulate the currents in both coils as a function of the gap and the force command. To illustrate this technique, consider the equation that describes the force exerted by the actuator:

$$F = K\left[\frac{I_1^2}{(g_o - \delta_g)^2} - \frac{I_2^2}{(g_o + \delta_g)^2}\right]$$

    where:

    g_o = nominal gap
    δg = gap motion
    I_1 = current in one actuator coil
    I_2 = current in the second coil
    K = force constant of actuator

    Now consider introducing a current into each actuator winding, which consists of a bias current and a current proportional to a commanded force, and multiplying the total current in winding 1 by $(g_o - \delta_g)$ and the total current in winding 2 by $(g_o + \delta_g)$. The force equation becomes:

$$F = K\left[\frac{(I_o + K_f F_c)^2 \frac{(g_o - \delta_g)^2}{g_o}}{(g_o - \delta_g)^2} - \frac{(I_o - K_f F_c)^2 \frac{(g_o + \delta_g)^2}{g_o}}{(g_o + \delta_g)^2}\right]$$

By selecting $K_f = g_o{}^2/4KI_o$, the force output becomes equal to the commanded force. Therefore, the actuator appears to be a linear device to the outer-loop control system. A block diagram of a circuit implementation is shown in Figure 14. This technique was used successfully on the AVS built for NASA's Langley Research Center.

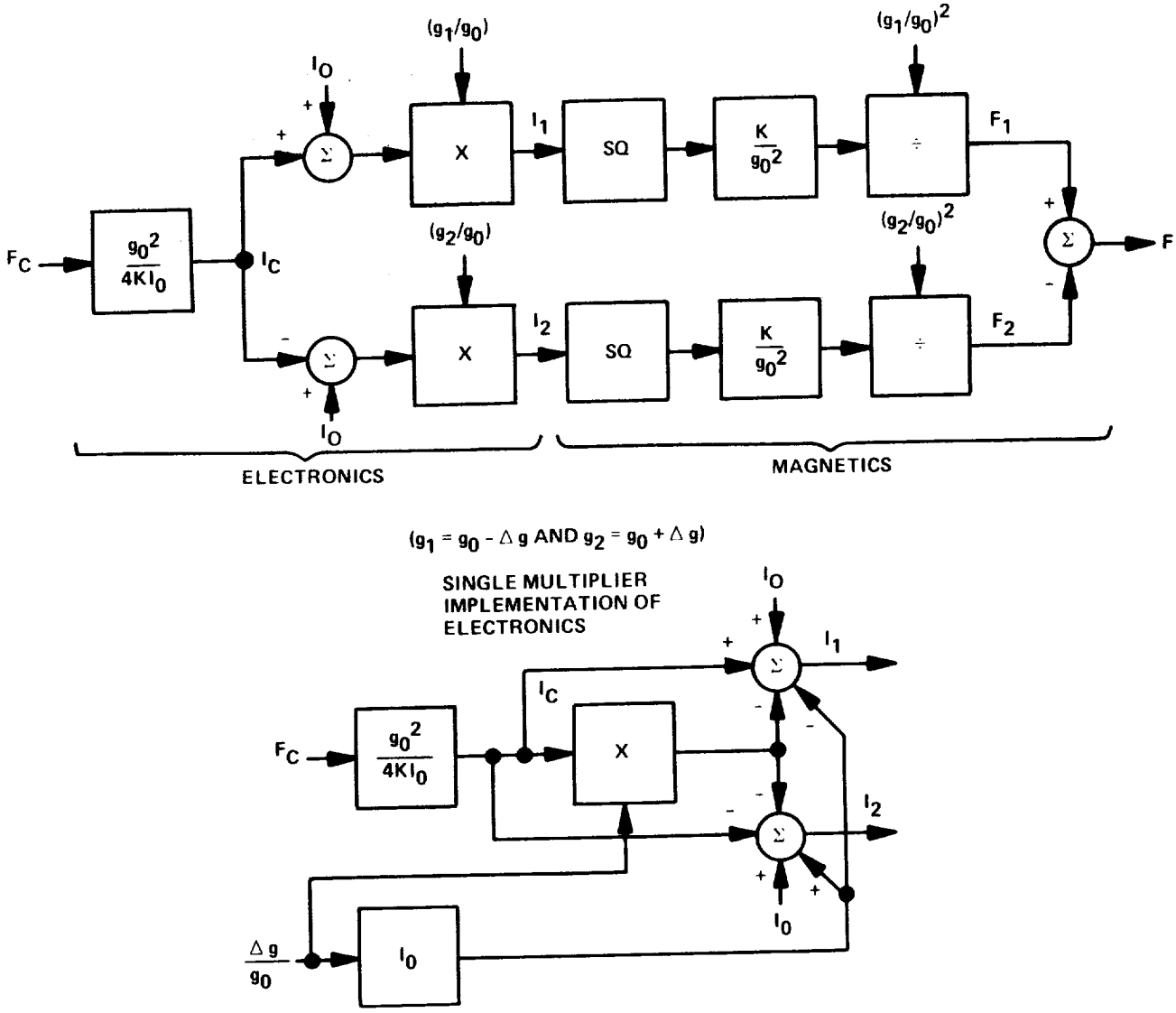

Figure 14. Current/Gap Force Linearization Technique

- Advantages/Disadvantages

The primary advantages of the gap/current technique are:

- The force produced is directly proportional to the commanded force.
- The electronics implementation is simple.

The disadvantages of the technique are:

- A gap sensor is required.
- A linear relationship between flux and current is required. Therefore, low-hysteresis iron must be used, which usually results in a heavy actuator because linear materials saturate at relatively low flux densities.
- The introduction of a bias current results in continuous power dissipation.

- Flux Feedback
  - Technique

The gap/current force equation has a dual in terms of flux. The force produced by the actuator is given by:

$$F = K(\lambda_1^2 - \lambda_2^2)$$

where:

λ_1 = flux linkage produced by magnet 1
λ_2 = flux linkage produced by magnet 2
K = force constant

Again, the actuator can be linearized by introducing a bias flux. Let $\lambda_1 = \lambda_o + K_f F_c$ and $\lambda_2 = \lambda_o - K_f F_c$. The force equation becomes:

$$F = K[(\lambda_o + K_f F_c)^2 - (\lambda_o - K_f F_c)^2] = 4\lambda_o K K_f F_c$$

If we let $\lambda_o = 1/4K$, we get $F = F_c$.

To implement flux feedback (Figure 15), flux is measured by a Hall-effect sensor. A high-bandwidth control loop is closed on the flux signal, creating a force actuator. The flux feedback technique has been used on the FEAMIS and the ISODRIVE and is currently the preferred control approach.

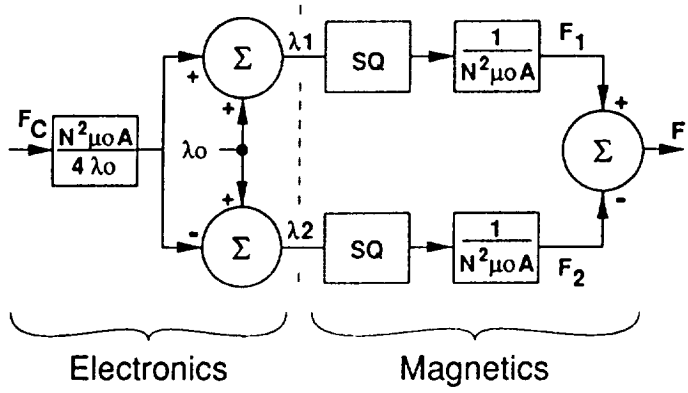

Figure 15. Flux Linearization Technique

  - Advantages/Disadvantages

Advantages of the flux feedback implementation are:

- Simple circuit implementation.
- Force produced is proportional to the commanded force.
- Because force produced by a magnet is directly proportional to the square of flux, the magnet can be made using high-hysteresis materials without affecting the linearity of the actuator. This feature results in a lighter, lower-power actuator.

The major drawback for this technique is that it requires a flux sensor that is linear and stable over temperature variations. It must also be placed within the air gap, making packaging a challenging task. Honeywell has developed circuit techniques that will compensate temperature for Hall-effect devices.

- Force Feedback
  - Technique
  - Force Feedback

    In applications that require a high-precision forcer, such as an isolation and pointing system, it becomes necessary to close an outer loop around the current loops (gap feedback) or the flux loops. The outer loop is closed by feeding back a measured value of the force applied to the payload. Figure 16 is a block diagram of the force loop and the required compensation.

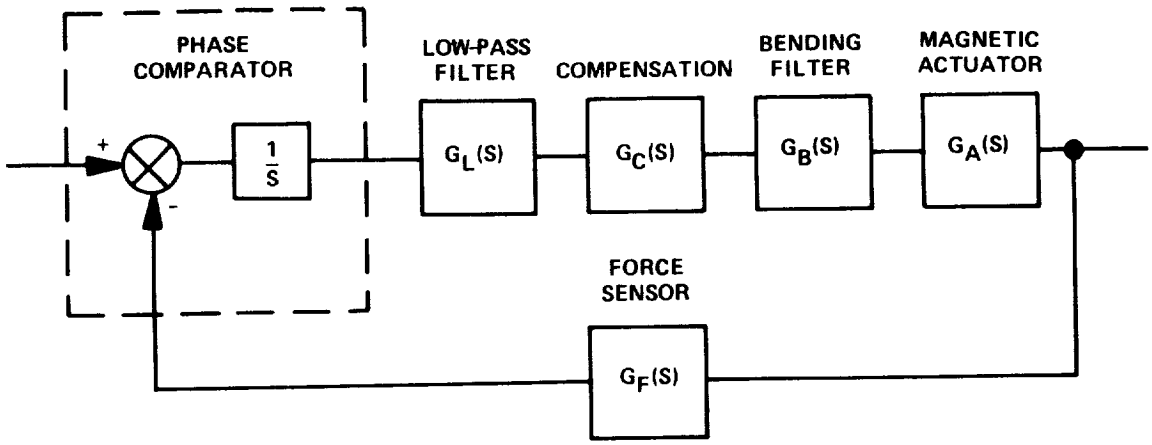

Figure 16. Force Feedback Control Loop

The force loop is an analog control loop. The precision force sensor employs a quartz crystal, which outputs a frequency-modulated signal representing the applied force. The additional circuitry required can be divided into three major functions: (1) the phase comparator and filter, (2) force-loop control compensation, and (3) a bending filter.

The phase comparator is used to differentiate the command- and frequency-modulated sensor frequencies. The particular logic circuit used is called a sequential frequency-phase detector. The output is a square wave that varies from a tristate level to high or low, depending on which frequency is higher; the duty cycle of the square wave is determined by the phase difference between the signals. This output is passed through a low-pass filter to extract the DC component containing the phase information and a level shifter to obtain a signal with polarity to drive the remainder of the control circuitry.

It is interesting to note the smooth transition that is made from digital to analog. The duty cycle (and hence the measured phase error) is a continuous function in the operating region; no sampling or quantization is introduced in the feedback path. The phase comparator also contributes a free integration that is used as part of the force-loop forward path.

The compensation for the force loop consists of an integrator and a lead/ lag filter. The integrator is added for two reasons. The first is to increase the system type to a Type 2. This forces the velocity error coefficient to infinity, which means that the loop will be able to follow ramp frequency commands. Secondly, the presence of the second integrator downstream from the phase comparator forces it to seek zero phase error in the steady state, thereby placing the nominal operating point in the center of the linear region. The double integrator in the forward path, along with higher frequency lags associated with those of comparator filter and the actuator, appears similar to a simple mass sytem. The lead/lag filter is added to stabilize the loop, using a standard form with displacement control loops.

The final element required is a bending mode (or notch) filter to decrease the effects of resonance associated with the force sensor. The sensor acts as a spring between the rotor and payload. Because the payload is much larger than the rotor, the natural frequency of this mass/spring system is determined by the rotor mass and sensor stiffness. This mode is lightly damped and occurs in the region from 100 to 130 Hz in the prototype sensors.

- Advantages/Disadvantages

The major advantage of force feedback is that extremely linear and accurate forces can be produced by the actuator. Force sensors utilizing quartz resonator techniques provide the necessary precise force measurement and stiffness. Drawbacks to the force sensor technique are:

- The relatively low stiffness of the force sensor limits achievable bandwidth of the actuator.
- The force sensor is rather fragile, necessitating complex and expensive mechanical mounting to provide protection.

When system considerations dictate extremely precise and linear forcers, the force feedback technique is the best choice.

TEST DATA

To verify the magnetic suspension isolation concept, tests have been run on a variety of hardware including single-degree-of-freedom and six-degree-of-freedom systems. This section briefly describes the tests conducted and provides samples of the results obtained.

To verify the magnetic suspension isolation concept, isolation tests were conducted using a linearized single-axis magnetic actuator [13]. The actuator was constructed from high-hysteresis, cold-rolled steel, and force was linearized using the flux-sensing technique.

To measure isolation performance, a low-frequency isolation loop was closed around the linearized actuator, using a capacitive position sensor. This sensor monitored the relative gap between the spacecraft-mounted assembly (stator) and the payload-mounted assembly (armature). This isolation loop was designed for a 10-Hz bandwidth with fifth-order rolloff.
A simplified block diagram of the system configuration is shown in Figure 17.

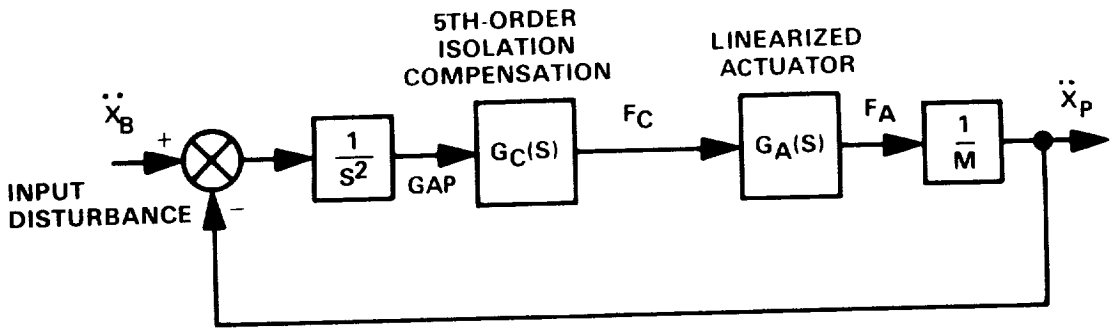

Figure 17. Simplified Magnetic Isolator Block Diagram

Prior to testing, dynamic modeling of the linearized actuator revealed that back emf and square-law linearization techniques inhibited ideal high-frequency rolloff of the isolation loop. These studies also indicated that the effects were related to the linearized actuator bandwidth and decreased as the actuator bandwidth increased. To demonstrate this phenomenon, the initial bandwidth of the linearized actuator was designed for 300 Hz and later increased to 600 Hz.

To measure the isolation properties of the magnetic isolator, the stator assembly was mounted to a sine-swept shaker to simulate spacecraft disturbance over frequency. The armature assembly consisted of a solid block and was suspended from the ceiling. The actuator test setup is shown in Figure 18. Because the actuator exerts force in only one axis, the remaining degrees of freedom were constrained by side ropes as shown.

Isolation data was measured using accelerometers (mounted on both the stator and armature assemblies) and recorded using a Hewlett Packard 5423A dynamic analyzer. Due to shaker and accelerometer limitations, the lowest recorded frequency of the measured data was 5 Hz.

The initial isolation results from the measured accelerometer signals are shown in Figure 19. Also shown is the anticipated response based on dynamic models of the linearized actuator, including the effects of back emf and bias linearization for a 300-Hz actuator. At frequencies below 60 Hz the measured data agrees with the anticipated results, demonstrating the 10-Hz isolation bandwidth, fifth-order rolloff, and as much as 80 dB of isolation; however, at frequencies above 60 Hz the deviation in the measured data was found to be caused by acoustic coupling. Sound waves from the shaker and stator during vibration impinged on the armature and were measured by the sensitive accelerometer.

To verify this phenomenon, the measurements were repeated with the isolation electronics disconnected. The measured transmissibility between the stator and armature accelerometers in this configuration is shown in Figure 20. Also shown are the anticipated results, the original measurement, and the difference of the two measurements as calculated by the dynamic analyzer. While somewhat noisy, the corrected data agrees with the anticipated results, thereby demonstrating that acoustic coupling is the source of degradation in the original measurement. To further improve measured isolation data, a technique was developed utilizing the flux feedback signals from the actuator. The difference between these signals is proportional to the applied

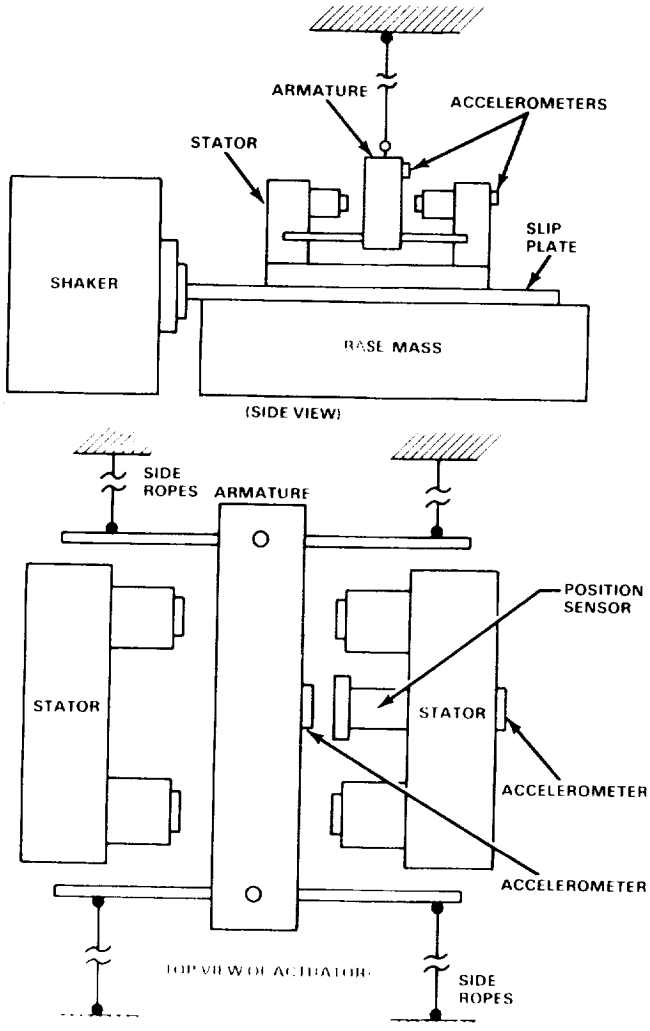

Figure 18. Magnetic Actuator Test Configuration

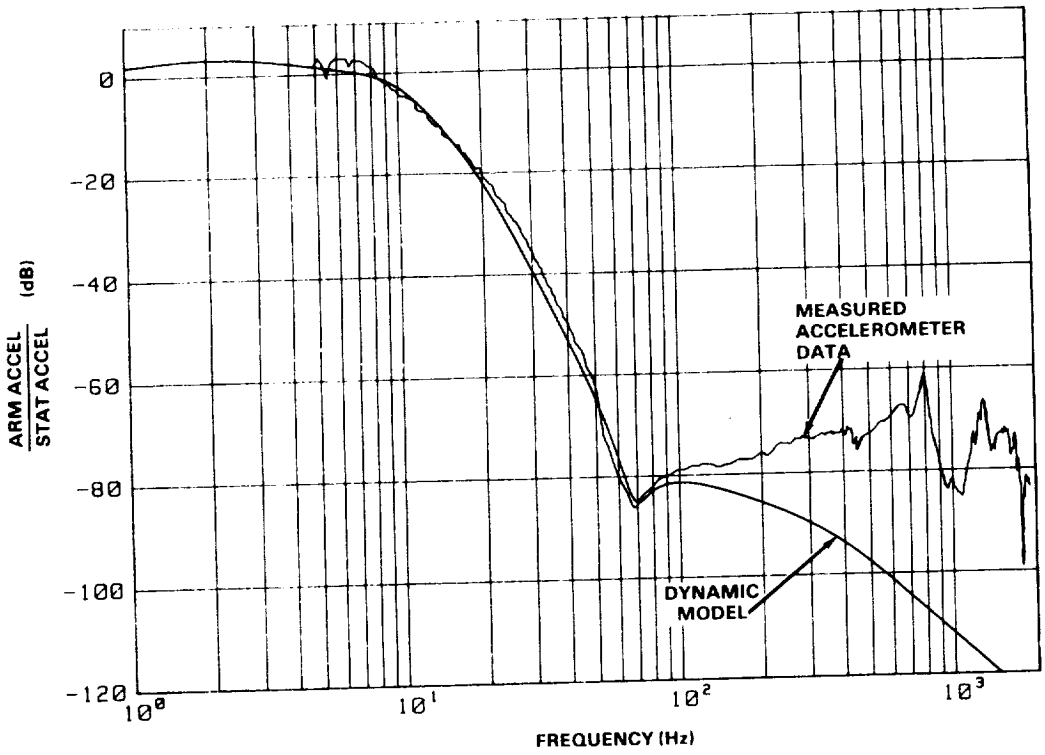

Figure 19. Comparison of Isolation Characteristics Between Measured Accelerometer Response and Dynamic Model Prediction

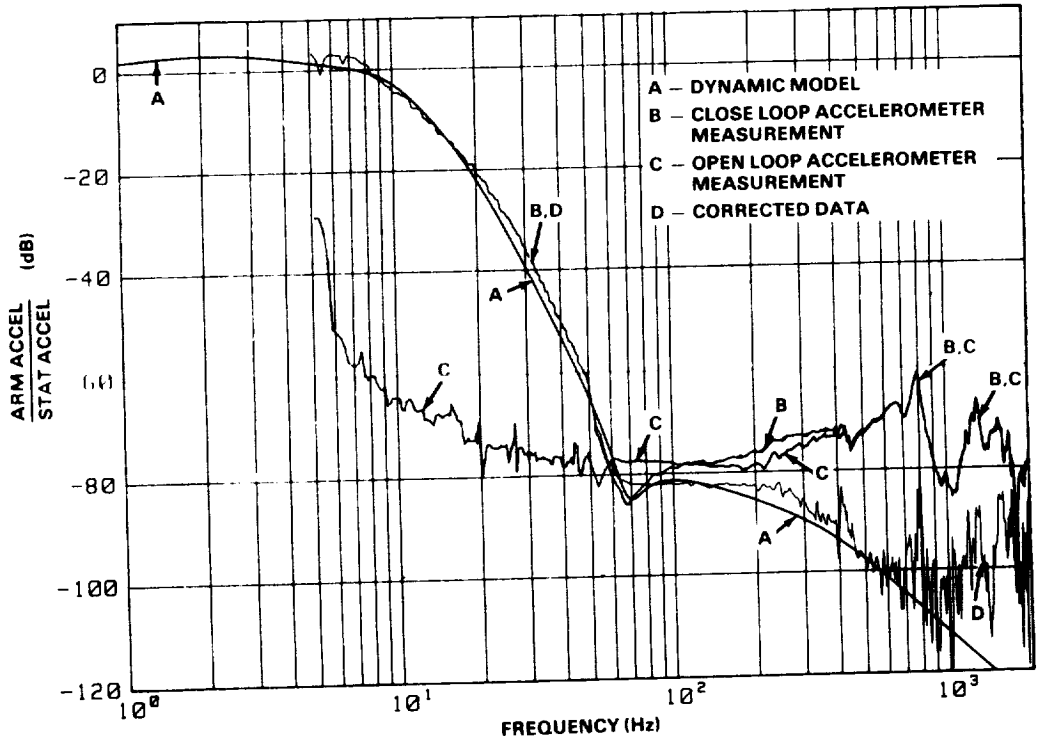

Figure 20. Isolation Characteristics Showing Results Corrected for Acoustics

force (i.e., acceleration) and is not affected by ambient acoustics. Using this flux feedback difference signal to measure armature acceleration, the isolation tests were repeated. The measured isolation response using this technique is shown in Figure 21, along with the anticipated results and corrected data from Figure 20. Note the improved signal and high correlation between this measurement and the corrected data results. The dip in the measured data (Figure 19) near 700 Hz is caused by a structural resonance in the stator assembly where one accelerometer was mounted. The leveling off near -90 dB above 1000 Hz is due to the electronic noise floor of the measurement equipment.

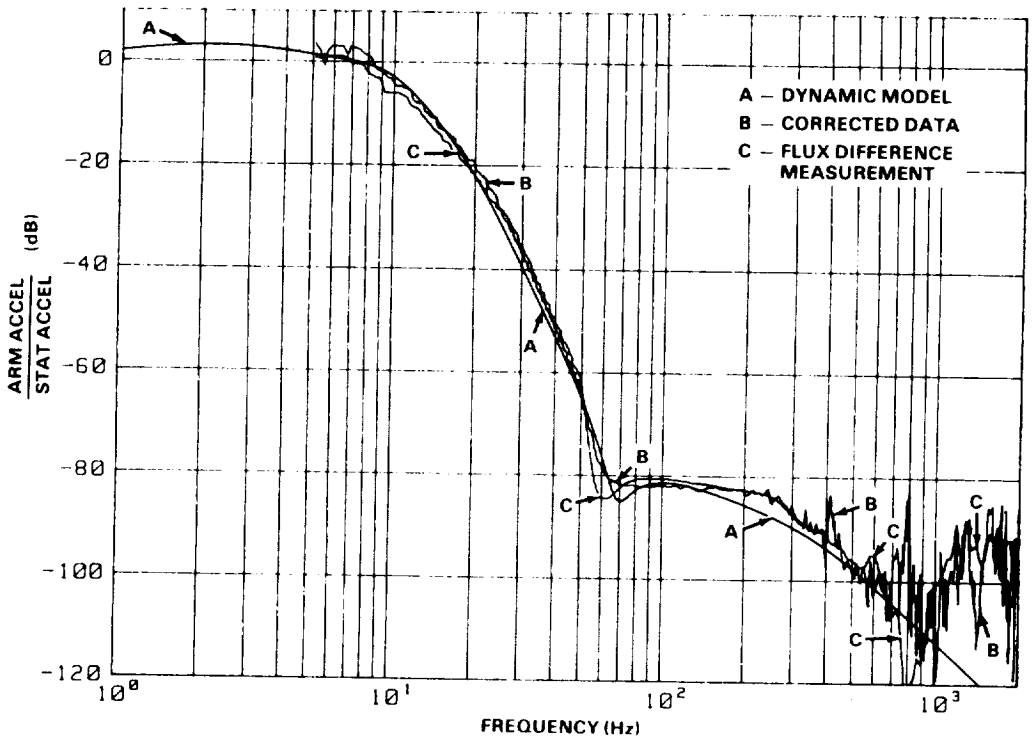

Figure 21. Isolation Characteristics Comparing Flux Difference Measurements to Corrected Data

To further verify the dynamic model and demonstrate how increasing the actuator bandwidth can improve the isolation characteristics, the actuator bandwidth was increased from 300 to 600 Hz, and the tests were repeated.

The measured and anticipated isolation characteristics for the 600-Hz configuration are shown in Figure 22. Also shown are the measured and anticipated characteristics for the 300-Hz actuator. Note the improved attenuation below 400 Hz. Here again, the leveling off near -90 dB is due to the electronic noise floor, and the dip near 700 Hz is due to stator structural resonance.

Test Summary

The single-axis magnetic isolator proved to exhibit excellent isolation characteristics, with as much as 90 dB of attenuation demonstrated to 2000 Hz. These tests also verified the accuracy of the dynamic model, which includes the anomalies due to back emf and bias linearization.

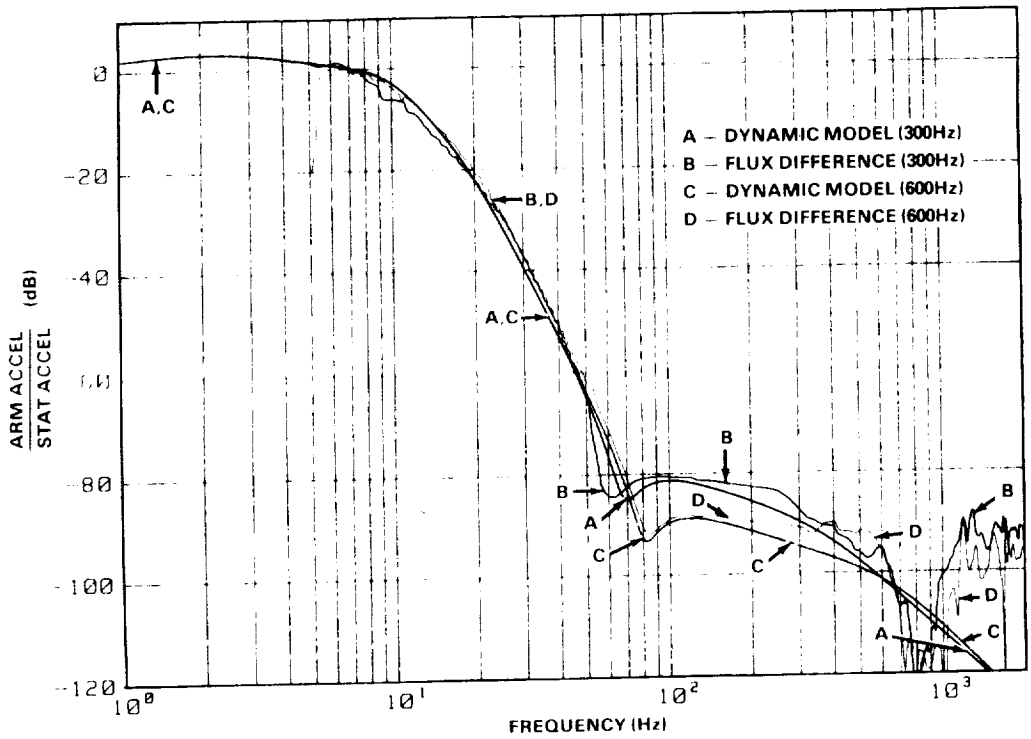

Figure 22. Isolation Characteristics Showing Effects of Increased Actuator Bandwidth

Since these tests were conducted, further improvements in the actuator bandwidths have been demonstrated in the laboratory, with bandwidths as high as 2000 Hz realized. In an isolation configuration, these high-bandwidth actuators would provide even higher attenuations than those presented here.

Advanced Vernier System (AVS)

The AVS has been extensively tested to prove its pointing capabilities [14]. Figure 23 is a photograph of the AVS test setup, and Figure 24 illustrates the equipment used to perform the testing. Because the gravity balance device corrupts the test data, a complete nonlinear simulation of the test setup was made. The results of the tests were compared with simulation runs to show analytical and test agreement. Of primary concern was the pointing error due to Shuttle Vernier Reaction Control System thruster disturbances. Simulated disturbances were applied to the AVS, and the response was measured. Figure 25 shows the result of one of these runs. Overall, the mean pointing error was 1.36 arc seconds versus an analytically predicted error of 1.22 arc seconds. This excellent agreement of data provides confidence that the techniques utilized to predict magnetic suspension pointing performance are sound.

FEAMIS

The test arrangement for FEAMIS is shown in Figure 26. The FEAMIS was mounted on a single-axis slip plate that was coupled to a linear shaker motor. A counterbalance arrangement offloaded the FEAMIS to allow it to levitate in a 1-g field. Accelerometers were mounted on the base and the simulated payload. The outputs of the two accelerometers were run into an HP5423 dynamics analyzer, and the transmissibility function was computed; Figure 27 shows the obtained transmissibility. The data compares with the predicted response and demonstrates 100-dB/decade rolloff and greater than 60-dB attenuation of high-frequency disturbances.

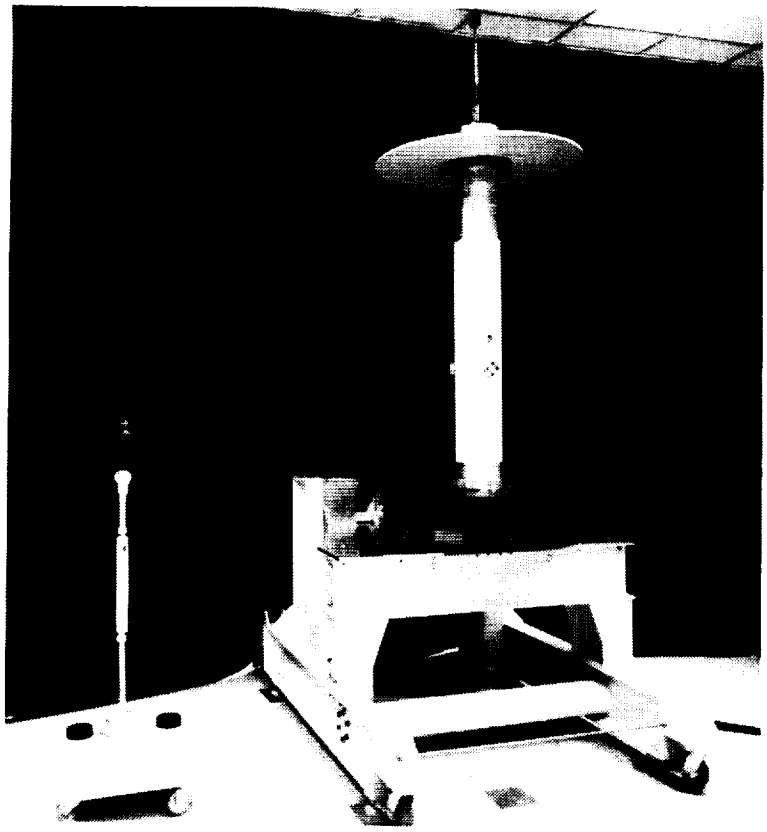

Figure 23. AVS with Suspended Payload Simulator

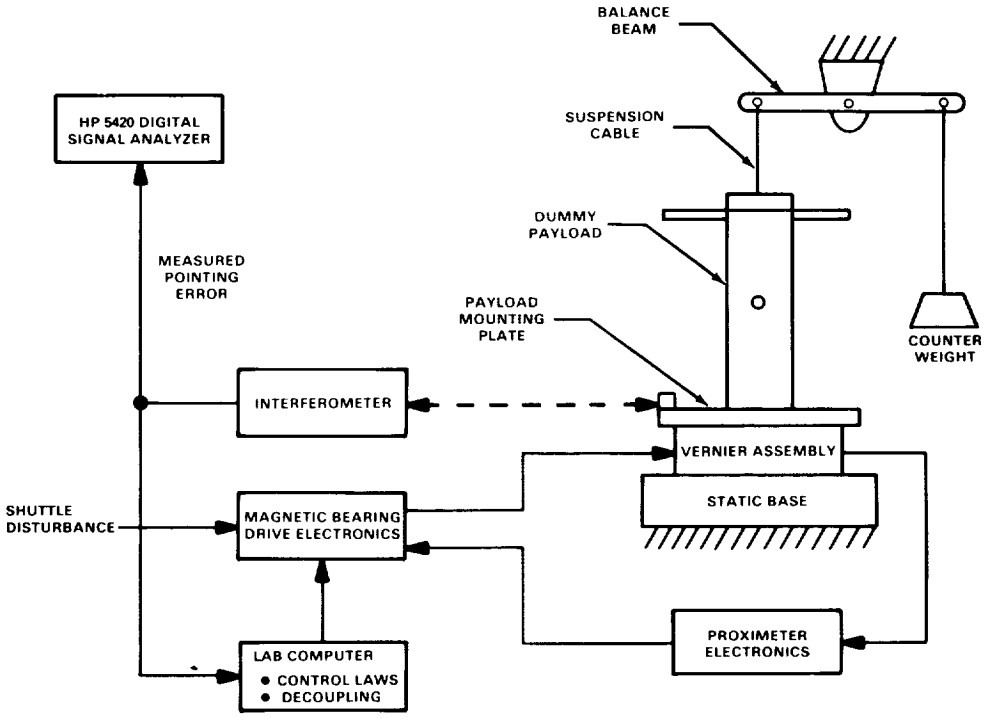

Figure 24. Laboratory Test Setup

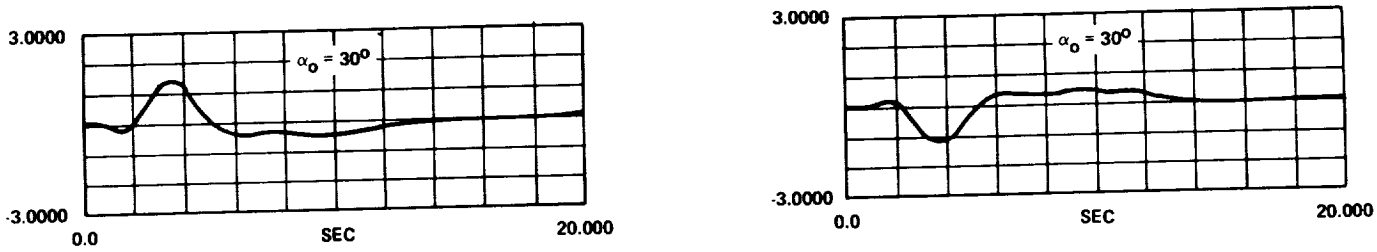

Figure 25. Pointing Error due to Simulated Shuttle VRCS Firing

ORIGINAL PAGE
BLACK AND WHITE PHOTOGRAPH

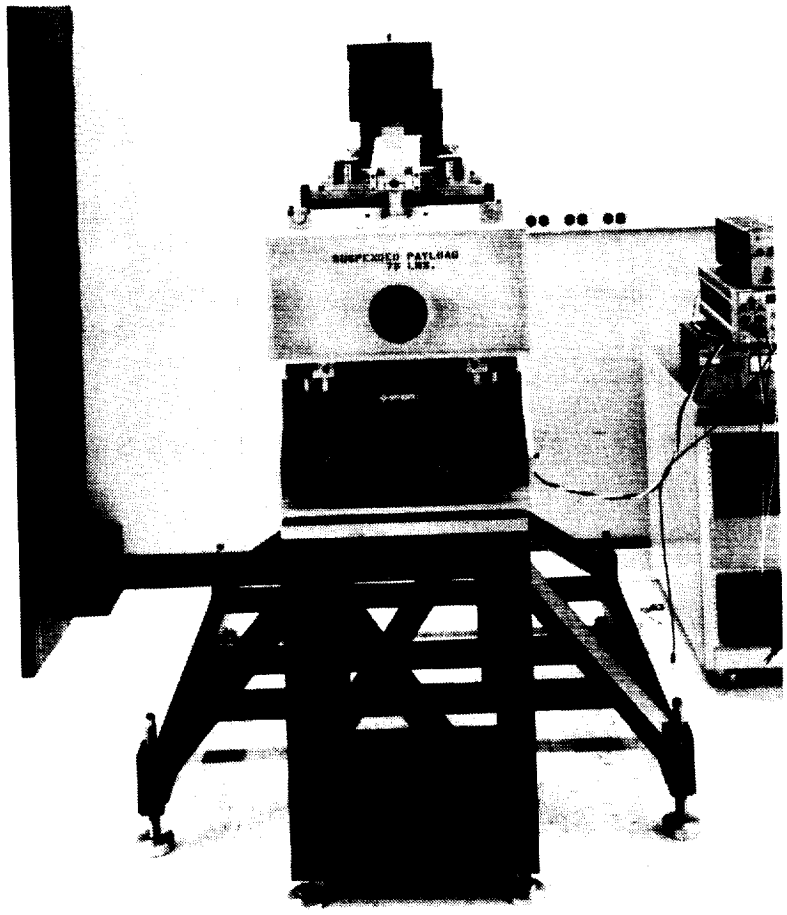

Figure 26. FEAMIS Test Setup

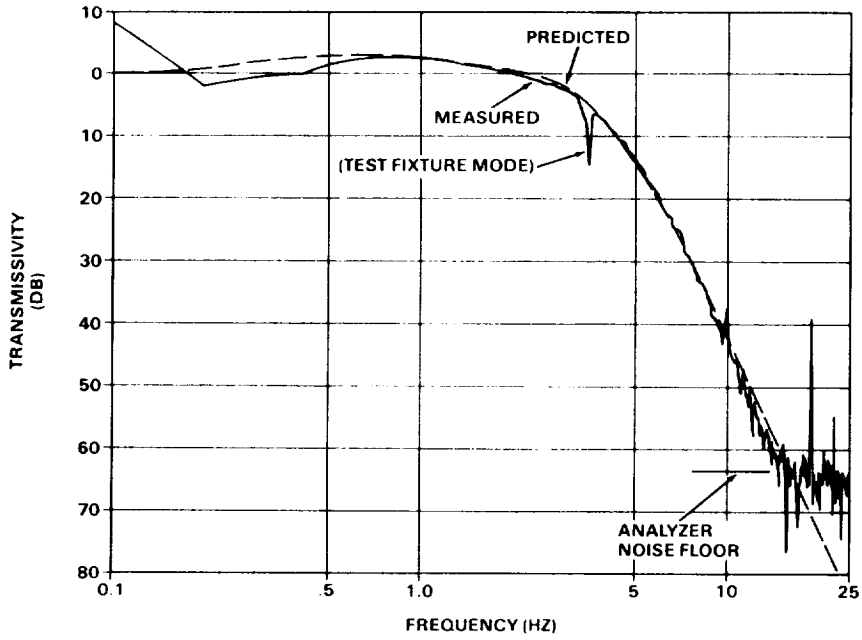

Figure 27. FEAMIS Isolation Characteristic

Conclusion

Honeywell's background in magnetic suspension technology has grown from a large diversity of programs. Extensive testing proves that magnetic suspension's noncontacting nature makes it uniquely suited for precision-pointing and isolation systems.

This wealth of experience and knowledge base has demonstrated that magnetic suspension systems for precision isolation and pointing of payloads in space is no longer a concept requiring significant development, but is a well-proven reality. What remains to be shown is the ultimate performance achievable in space with a flight demonstration.

REFERENCES

1. W.W. Anderson and S.M. Joshi. "The Annular Suspension and Pointing (ASP) System for Space Experiments and Predicted Pointing Accuracies." NASA TR R-488, December 1975.

2. W.W. Anderson and N.J. Groom. "Magnetic Suspension and Pointing System." U.S. Letters Patent No. 4,088,018, May 9, 1978.

3. W.W. Anderson and N.J. Groom. "Magnetic Suspension and Pointing System." U.S. Letters Patent No. 4,156,548, May 29, 1979.

4. D.C. Cunningham, T.P. Gismondi, and G.W. Wilson. "System Design of the Annular Suspension and Pointing System (ASPS)." AIAA Paper 78-1311, Palo Alto, CA, August 1978.

5. C.R. Keckler, K.S. Kibler, and L.F. Rowell. Determination of ASPS Performance for Large Payloads in the Shuttle Orbiter Disturbance Environment. NASA TM-80136, October 1979.

6. W.W. Anderson, N.J. Groom, and C.T. Woolley. "Annular Suspension and Pointing System." Article No. 78-1319R, Journal of Guidance and Control, Vol. 2, No. 5, September 1979.

7. D.C. Cunningham, et al. Design of the Annular Suspension and Pointing System. NASA CR-3343, January 1980.

8. R.V. VanRiper. "A Precision Pointing System for Shuttle Experiment Payloads." 17th Space Congress, May 1980.

9. R.V. Van Riper. "High Stability Shuttle Pointing System." SPIE Paper 265-12, Los Angeles Technical Symposium, February 1981.

10. T. Allen, D.D. Havenhill, and K.D. Kral. "FEAMIS: A Magnetically Suspended Isolation System for Space-Based Materials Processing." Annual AAS Guidance and Control Conference, February 1986.

11. B.J. Hamilton. "Stability of Magnetically Suspended Optics in a Vibration Environment." SPIE Paper 295-21, San Diego Technical Symposium, August 1981.

12. B.J. Hamilton. "Magnetic Suspension: The Next Generation in Precision Pointing." AAS Paper 82-034, Rocky Mountain Guidance and Control Conference, February 1982.

13. D.D. Havenhill and K.D. Kral. "Payload Isolation using Magnetic Isolation." AAS Paper 85-014, Rocky Mountain Guidance and Control Conference, February 1985.

14. B.J. Hamilton. Laboratory Evaluation of the Pointing Stability of the ASPS Vernier System. NASA CR-159307, June 1980.

15. J. Sellers. Impact of Magnetic Isolation on Pointing Performance in the Presence of Structural Flexibility. NASA CR-172481, February 1985.